

CERN-EP-2023-265

17 November 2023

Emergence of long-range angular correlations in low-multiplicity proton–proton collisions

ALICE Collaboration*

Abstract

This Letter presents the measurement of near-side associated per-trigger yields, denoted ridge yields, from the analysis of angular correlations of charged hadrons in proton–proton collisions at $\sqrt{s} = 13\text{ TeV}$. Long-range ridge yields are extracted for pairs of charged particles with a pseudorapidity difference of $1.4 < |\Delta\eta| < 1.8$ and a transverse momentum of $1 < p_T < 2\text{ GeV}/c$, as a function of the charged-particle multiplicity measured at midrapidity. This study extends the measurements of the ridge yield to the low multiplicity region, where in hadronic collisions it is typically conjectured that a strongly-interacting medium is unlikely to be formed. The precision of the new results allows for the first direct quantitative comparison with the results obtained in e^+e^- collisions at $\sqrt{s} = 91\text{ GeV}$, where initial-state effects such as pre-equilibrium dynamics and collision geometry are not expected to play a role. In the multiplicity range where the e^+e^- results have good precision, the measured ridge yields in pp collisions are substantially larger than the limits set in e^+e^- annihilations. Consequently, the findings presented in this Letter suggest that the processes involved in e^+e^- annihilations do not contribute significantly to the emergence of long-range correlations in pp collisions.

Long-range angular correlations have been observed in the collisions of ultra-relativistic heavy ions both at RHIC [1–4] and LHC [5–7]. In such collisions, the presence of correlations between pairs of particles with large pseudorapidity differences is interpreted as a signature for the existence of a strongly-coupled medium, known as the quark–gluon plasma (QGP), which converts the initial pressure gradients created in non-central nucleus–nucleus collisions into a collective momentum anisotropy of the final-state hadrons. In particular, the collectivity signal manifests itself as a near-side ridge around the jet fragmentation peak in the two-particle correlation function, indicating the presence of a medium with considerable anisotropic flow.

Long-range correlations have also been observed in high-multiplicity proton–proton (pp) [8–12], proton–nucleus (pA) [13–16], and light nucleus–nucleus collisions [17, 18]. These results have challenged the interpretation of the so-called collective phenomena in hadronic collisions, and raised the question whether the same underlying dynamics can be responsible for the emergence of long-range correlations in small and large systems [19]. Notably, the formation of a medium and its subsequent evolution, which is understood to take place in heavy-ion collisions might not be justifiable in small collision systems, where the requirement of thermal equilibrium may not be achieved under the conditions of small system size. Despite a vast experimental and theoretical effort, an unambiguous description of these experimental data is not yet achieved [20–22], although there has been recent progress [23–25]. Flow-like signatures could indeed originate from the very early stages of the collisions [26, 27] or develop during the late stages of the collisions as a consequence of the interaction with a strongly-coupled medium [28, 29]. This suggests that ridge measurements combined with measurements of jet shape modification can eventually be used to separate initial state and flow-driven contributions [30].

Recently, new experimental insights have been obtained by the study of long-range correlations in e^+e^- collisions at $\sqrt{s} = 91\text{ GeV}$ using ALEPH [31] archived data [32]. Collisions between point-like electrons and positrons remain unaffected by the presence of beam remnants or gluonic initial-state radiation, and are not sensitive to the modeling of parton distribution functions [33, 34]. Near-side ridge is neither observed in the lab reference frame nor in the thrust-axis reference frame. The results obtained in e^+e^- collisions were also compared with the associated yield measurement in pp collisions with CMS [35, 36], but due to the large uncertainties of the existing pp measurement, a statistically significant comparison between the ridge yields measured in pp and e^+e^- collisions was not feasible. A systematic study of such signatures across collision systems and sizes represents a unique opportunity to characterize the emergence of collective phenomena. In particular, measurements performed in pp collisions with very low multiplicity can provide crucial inputs to address the relevance of initial-state effects [28] in the presumed absence of a flow-inducing medium and final-state correlations [37, 38], and in turn constrain the magnitude of these effects traditionally afflicted by a large uncertainty [39]. At the same time, comparing to the e^+e^- collision system helps to identify physical processes in the pp system that do contribute to collectivity, as no such signals were detected in the e^+e^- system [32].

In this Letter, the near-side long-range yields are measured in pp collisions at $\sqrt{s} = 13\text{ TeV}$ with good precision down to very low multiplicities. The results are reported for pairs of charged particles with pseudorapidity $1.4 < |\Delta\eta| < 1.8$ and transverse momentum $1 < p_T < 2\text{ GeV}/c$, as a function of the charged-particle multiplicity measured at midrapidity. The experimental precision of this study allows for the first quantitative comparison with the results obtained in e^+e^- collisions at $\sqrt{s} = 91\text{ GeV}$ with ALEPH archived data, where initial-state effects are not expected to play a role. The measurement is also compared to predictions of PYTHIA 8.3 [38] and EPOS LHC simulations [40].

The data were collected in 2017 and 2018 using the ALICE apparatus [41] at the LHC. Information about the detector configuration and performance can be found in Refs. [42, 43]. The main systems used for this study were the central-barrel detectors, located within a solenoidal magnet and used for charged-particle tracking. These include the Inner Tracking System and the Time Projection Chamber. The V0 detector, consisting of two scintillator arrays located at pseudorapidities of $2.8 < \eta < 5.1$ and

$-3.7 < \eta < -1.7$, was used for the trigger and event selections. Minimum-bias (MB) events were selected online by requiring a signal from at least one charged particle in both V0 counters. The analyzed data sample consists of about 1.3 billion MB pp collisions at a center-of-mass energy of $\sqrt{s} = 13\text{ TeV}$ within primary vertex range $z_{\text{vtx}} < 8.0\text{ cm}$ along the beam axis, corresponding to an integrated luminosity of about 22 nb^{-1} .

The observables presented in this analysis are extracted using two-particle angular correlations for pairs of charged particles. The two-particle per-trigger yield is measured as a function of relative azimuthal angle $\Delta\varphi$ and pseudorapidity $\Delta\eta$ of two particles – traditionally called trigger and associated – and is defined as

$$\frac{1}{N_{\text{trig}}} \frac{d^2N_{\text{pair}}}{d\Delta\eta d\Delta\varphi} = B(0,0) \frac{S(\Delta\eta, \Delta\varphi)}{B(\Delta\eta, \Delta\varphi)}. \quad (1)$$

Eq. (1) is evaluated within a range of transverse momentum of the trigger ($p_{T,\text{trig}}$) and associated ($p_{T,\text{assoc}}$) particles within $|\eta| < 1.0$ where $p_{T,\text{trig}} > p_{T,\text{assoc}}$. The total number of trigger particles is denoted with N_{trig} , and the number of trigger and associated particle pairs with N_{pair} . This two-particle yield $S(\Delta\eta, \Delta\varphi)$ is corrected for pair acceptance and reconstruction effects by constructing a mixed-event distribution $B(\Delta\eta, \Delta\varphi)$ from pairs where the trigger and associated particles are taken from different events. This mixed-event distribution is normalized by $B(0,0)$ computed by pairs of like-sign particles traveling in the same direction for which acceptance and reconstruction effects are identical by construction. The event mixing is performed such that events with similar multiplicity and primary vertex z_{vtx} (bins of 2 cm) are combined. The final per-trigger yield is obtained by averaging over these individual bins. In addition, all tracks are corrected for the single-particle tracking efficiency as a function of p_T and η . The efficiency corrections and acceptance factors are obtained by simulating events with PYTHIA 8.3 with the Monash tune [44], and the detector response simulated using the GEANT3 transport package [45].

The per-trigger yield distribution as a function of $\Delta\varphi$ is obtained by integrating the two-dimensional two-particle per-trigger yield in the long-range intervals $1.4 < |\Delta\eta| < 1.8$, in order to exclude the region dominated by the jet fragmentation peak

$$Y(\Delta\varphi) = \frac{1}{N_{\text{trig}}} \frac{dN_{\text{pair}}}{d\Delta\varphi} = \int_{1.4 < |\Delta\eta| < 1.8} \left(\frac{1}{N_{\text{trig}}} \frac{d^2N_{\text{pair}}}{d\Delta\eta d\Delta\varphi} \right) \frac{1}{\delta_{\Delta\eta}} d\Delta\eta, \quad (2)$$

where $\delta_{\Delta\eta} = 0.8$ is the normalization constant for the chosen $\Delta\eta$ range. The ridge yield Y^{ridge} is extracted by integrating the near-side area of the associated per-trigger yield using

$$Y^{\text{ridge}} = \int_{|\Delta\varphi| < |\Delta\varphi_{\min}|} Y(\Delta\varphi) d\Delta\varphi - 2|\Delta\varphi_{\min}| C_{\text{ZYAM}}. \quad (3)$$

A Zero-Yield-At-Minimum (ZYAM) procedure is applied to subtract the baseline of the per-trigger yield. We assume that $Y(\Delta\varphi)$ has an uncorrelated flat contribution, $C_{\text{ZYAM}} = Y(\Delta\varphi_{\min})$, where $\Delta\varphi_{\min}$ is the location of the minimum of $Y(\Delta\varphi)$. To reduce the impact of statistical fluctuations, $Y(\Delta\varphi)$ is fitted by a symmetric Fourier series up to third harmonic $F(\Delta\varphi) = \sum_{n=0}^3 2a_n \cos(n\Delta\varphi)$, which is found to be adequate for a precise extraction of $\Delta\varphi_{\min}$ and C_{ZYAM} . This procedure is illustrated in the right panel of Fig. 1. Since the fit is only used to locate the bounds of the near-side ridge, the impact of the higher harmonics on the baseline and ZYAM procedure is negligible. The ridge yield provides a measure for collective effects, and is generally compatible with the measurements of flow coefficients v_n in small systems [46]. The measurement of Y^{ridge} also facilitates the comparison with the readily available e^+e^- result, and does not suffer from ambiguities related to low-multiplicity template subtraction applied in other measurements [15].

The analysis is performed in different intervals of measured multiplicity. In order to determine the corrected charged-particle multiplicity $\langle N_{\text{ch}} \rangle$ in each multiplicity interval, the number of charged tracks is

counted within $|\eta| < 1$ and $p_T > 0.2 \text{ GeV}/c$. This number is corrected for detector effects by correlating reconstructed and simulated multiplicities, and randomly sampling a new multiplicity value from the simulated distribution corresponding to the reconstructed value. At the same time, the resampling technique reduces self-correlation between the multiplicity and the particles entering the per-trigger yield. The analysis is carried out for 14 multiplicity intervals, ranging from $N_{\text{ch}} = 0$ to 62, where the average MB multiplicity is about 11.3.

The systematic uncertainties of the ridge yields are evaluated by varying the event and track selections as well as the integration ranges used in the extraction. A bootstrapping procedure [32] is used to estimate both the statistical and systematic uncertainties. For multiplicity intervals where the result is consistent with zero, a limit is estimated at 95% confidence level (CL). This limit is obtained by making several variations of the default value $Y_{\text{def}}(\Delta\phi)$ of the per-trigger yield distribution, by adding random statistical and systematic fluctuations and extracting the ridge yield applying the procedure as given in Eq. (3). Gaussian fluctuations are randomly added bin-by-bin based on the statistical uncertainty. Systematic fluctuations are included by assuming that the $Y_s(\Delta\phi)/Y_{\text{def}}(\Delta\phi)$ variation for each source of systematic uncertainty s has a common shift across $(\Delta\phi, \Delta\eta)$ (not affecting the ridge yield) and a bin-by-bin component, taken to be Gaussian distributed and each variation corresponding to 1σ . It should be noted that the statistical uncertainties and the five sources of systematic uncertainty described below are all varied each time. The final uncertainty on Y^{ridge} is calculated as the standard deviation of the yield distribution obtained from a large number of these random variations.

The selection on the position of the primary vertex along the beam axis (z_{vtx}) is varied from $|z_{\text{vtx}}| < 8 \text{ cm}$ to 10 cm. The corresponding systematic uncertainty was found to be less than 5% depending on multiplicity. In order to estimate the bias due to the possible presence of jet-like correlations in $1.4 < |\Delta\eta| < 1.8$, the definition of the long-range region was changed to $1.5 < |\Delta\eta| < 1.8$. This change also estimates the effect of residual non-flow in the region in which the ridge yield is extracted. As the near-side ridge yield decreases towards low multiplicity, the relative contribution to the systematic uncertainty increases from 3% at high multiplicity to 22% at $\langle N_{\text{ch}} \rangle = 15$, and dominates for lower multiplicity. Uncertainties related to track reconstruction were estimated by varying the required number of hits in the ITS layers allowing a more uniform detector acceptance but larger contributions from secondaries, resulting in 3–10% variation without a clear multiplicity dependence. Residual two-particle acceptance effects due to the finite accuracy of the event-mixing pair-acceptance correction, generally affecting the structure at long-range $\Delta\eta$, have been estimated to be around 4% on average. This contribution has been evaluated by adjusting the per-trigger yield with a $\Delta\phi$ -independent factor such that the away-side region is constant over $\Delta\eta$. As an additional check on the extraction of the associated yield, the $\Delta\phi$ integration region is shifted with a resulting difference of about 1%. The total systematic uncertainty resulting from the bootstrapping procedure is around 15% at high multiplicities and 30% at low multiplicities.

Figure 1 presents the two-particle per-trigger yield for trigger and associated particle momentum of $1 < p_T < 2 \text{ GeV}/c$ in the multiplicity interval $32 < N_{\text{ch}} \leq 37$. A prominent jet-fragmentation peak originating from correlations of particles from the fragmentation of the same parton is visible at $(\Delta\eta, \Delta\phi) = (0, 0)$. At $\Delta\phi = \pi$, a broad away-side structure results from correlations of tracks from back-to-back jet-fragments that are spread over the entire $\Delta\eta$ -region (as the parton–parton scattering center-of-mass frame is not the lab frame). The momentum region has been chosen such that these peaks are sufficiently narrow in $\Delta\phi$, allowing one to extract the long-range ridge yield. At $|\Delta\eta| \gtrsim 1.4$ and $\Delta\phi \approx 0$, the “ridge” structure is visible which was observed in previous measurements [47] and that in heavy-ion collisions is interpreted as a sign of collective expansion of the QGP medium.

Figure 2 shows the extracted ridge yield Y^{ridge} as a function of the average charged-particle multiplicity. The measured Y^{ridge} shows a strong multiplicity dependence, with an increasing trend towards higher multiplicity collisions. A non-zero Y^{ridge} is measured with good precision for events with $\langle N_{\text{ch}} \rangle > 9$, significantly extending the low-multiplicity reach of previous measurements [35]. A limit, represented in

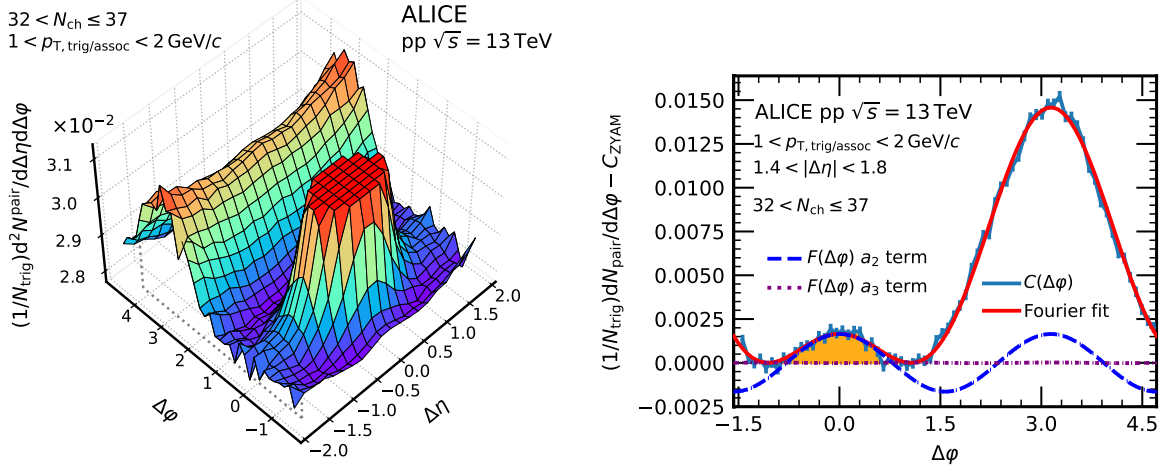


Figure 1: Two-particle per-trigger yield measured for charged track pairs with $1 < p_{\text{T},\text{trig}} < 2 \text{ GeV}/c$ and $1 < p_{\text{T},\text{assoc}} < 2 \text{ GeV}/c$ within the multiplicity range $32 < N_{\text{ch}} \leq 37$. The jet fragmentation peak has been truncated to ensure a better visibility of the long-range structure. The right panel shows the zero-suppressed projection to $\Delta\varphi$ overlaid with $F(\Delta\varphi)$ (red line) and the area in which the ridge yield is extracted (shaded area). The blue and purple lines represent the second and third harmonic terms of $F(\Delta\varphi)$.

the figure by the black arrows, is computed at 95% CL for the three lowest multiplicity intervals ($\langle N_{\text{ch}} \rangle < 9$) where no significant ridge yield was observed. The origin of the arrow corresponds to the threshold value of the ridge yield ($Y_{\text{CL}}^{\text{ridge}}$) for which 95% of the bootstrap distribution values are smaller than $Y_{\text{CL}}^{\text{ridge}}$. The results are compared with an analogous measurement performed by CMS (green markers) at the same center-of-mass energy. To allow for a direct comparison with the ALICE measurement, the x -axis of the CMS data was scaled by the ratio of the pseudorapidity acceptance of CMS and ALICE, which was estimated to be about 0.66 with negligible statistical uncertainty based on PYTHIA 8.3 simulations. The CMS result presents finite near-side yields for $\langle N_{\text{ch}} \rangle \gtrsim 38$ and limits at 67% CL for smaller multiplicities. The two results are in good agreement at high multiplicities, where an accurate estimation of the ridge yields is available for both experiments. The comparison also includes CMS measurements at $\sqrt{s} = 7 \text{ TeV}$. The measurement at $\sqrt{s} = 7 \text{ TeV}$ has a smaller uncertainty at $\langle N_{\text{ch}} \rangle \sim 32$ compared to the one at $\sqrt{s} = 13 \text{ TeV}$ and also agrees with the ALICE results.

In Fig. 3, the result is compared to a recent measurement performed in e^+e^- collisions at $\sqrt{s} = 91 \text{ GeV}$ in the thrust-axis reference frame using ALEPH archived data [32], where no evidence of long-range near-side correlations was observed. Due to the absence of beam remnants, the thrust axis provides an estimate of the longitudinal color field between the initially created $q\bar{q}$ pair and is therefore the sensible choice in e^+e^- collisions to search for collective effects. Similarly to the previous figure, in order to translate the ALEPH multiplicity into the ALICE acceptance range, a scaling factor is estimated with PYTHIA 8.3 events by counting the resulting particles in the acceptance ranges of both experiments ($|\eta| < 1.738$, $p_{\text{T}} > 0.2 \text{ GeV}/c$ in case of ALEPH). It is inherently difficult to compare the multiplicity in these two collision systems which have more than two orders of magnitude difference in collision energy as well as a different initial state leading to different flavour composition as well as multiplicity and momentum distributions. In order to give justice to these differences, this procedure was performed in both pp collisions at $\sqrt{s} = 13 \text{ TeV}$ and e^+e^- collisions at $\sqrt{s} = 91 \text{ GeV}$ with resulting correction coefficients $c_{\text{pp}} = 0.57$ and $c_{ee} = 0.78$, respectively. The large difference between these two estimations reflects the different underlying mechanisms leading to multiplicity production in pp and e^+e^- collisions and is depicted by the horizontal uncertainty bars of the ALEPH ridge yields which are given as limits at 95% CL. In the multiplicity range 8 to 18 the yields in pp collisions are substantially above the ALEPH limit while outside this range the limits from e^+e^- collisions are above the pp measurement.

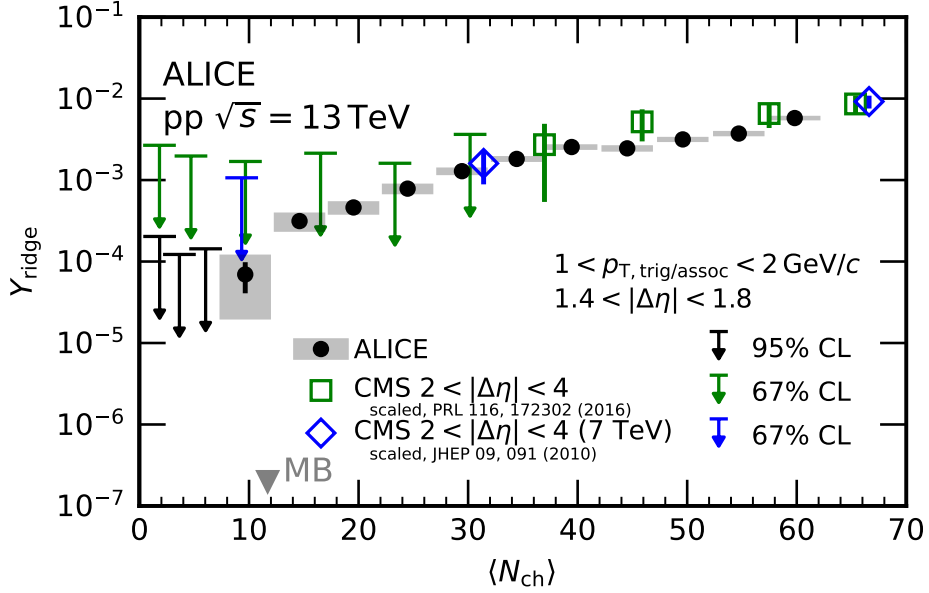


Figure 2: Ridge yield as a function of multiplicity. The black points correspond to the measurement presented in this Letter, while data from CMS [35] are drawn as green and blue markers. Vertical bars denote statistical uncertainties while systematic uncertainty is shown as shaded area. For both results, at low multiplicity where the lower uncertainty reaches zero, an upper limit is reported, which is drawn as a bar and arrow-down. Such points are given at 95% CL for the results from this Letter and at 67% for the results from CMS. The “MB” arrow indicates the multiplicity averaged over the entire considered multiplicity range.

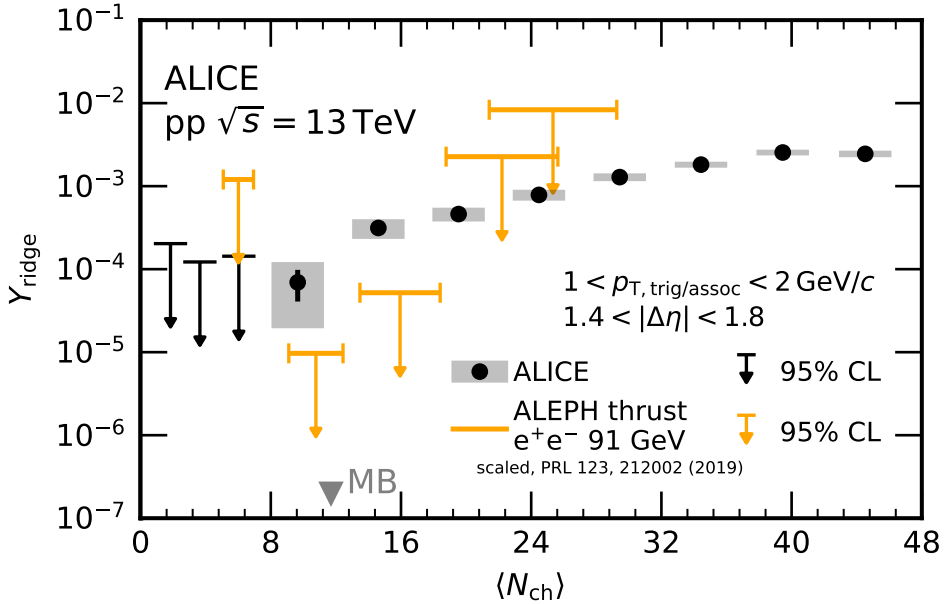


Figure 3: Ridge yield as a function of multiplicity, compared to the upper limits on the ridge yield in e^+e^- collisions. Vertical bars denote statistical uncertainties while systematic uncertainty is shown as shaded area. The orange limits represent the measurement in the thrust-axis reference frame with ALEPH [32]. The horizontal bars in the ALEPH points represent the uncertainty related to the multiplicity conversion from the ALEPH to the ALICE acceptance (see text). All limits are given at 95% CL.

In order to quantify this finding the significance of the result in pp collisions to be above the one in e^+e^- collisions is computed. The ALICE result is linearly interpolated between the two closest points

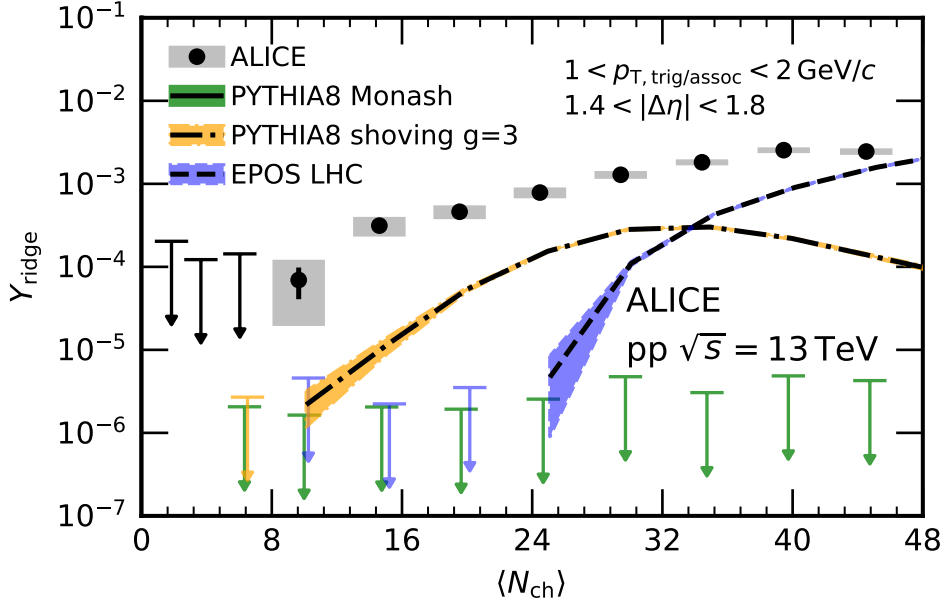


Figure 4: Ridge yield as a function of multiplicity compared to the predictions of PYTHIA 8.3 [38] with Monash tune [44] (green) and string shoving ($g = 3$) [48] as well as EPOS LHC simulations [40] (blue). Due to a larger jet fragmentation peak width in the simulations than in data, the yield is extracted within $2 < |\Delta\eta| < 4$ for the model calculations. A 95% CL is indicated for model calculations when the lower limit of statistical uncertainty is below zero. Some points are slightly displaced along the x -axis for better visualization. The band indicates the statistical uncertainty from the event generation and the extraction procedure.

to match the multiplicity. Statistical and systematic uncertainties contribute about equally and the results at different multiplicities are combined assuming the systematic uncertainty to be fully correlated across multiplicity intervals. The resulting significance of the pp measurement to be above the one in e^+e^- collisions is 3.8σ (using c_{pp}) and 5.0σ (using c_{ee}). Due to the precision of the ALEPH measurement, the multiplicity range which contributes mostly is between 8 and 18. Computing the significance separately in this range results in, for c_{pp} , a compatibility of 1.5σ and 3.2σ for the two ALEPH measurements within this multiplicity range, while c_{ee} yields 2.9σ and 4.4σ , respectively. This significant difference in the multiplicity range 8 to 18, where a near-side ridge is clearly present in pp collisions, suggests that the processes involved in e^+e^- annihilations do not contribute significantly to the emergence of long-range correlations in pp collisions.

In Fig. 4, the near-side yields are compared to the predictions of PYTHIA 8.3 with the Monash tune [44] and the string shoving tune ($g = 3$) [48], as well as EPOS LHC calculations. For the model calculations, a long-range definition of $2 < |\Delta\eta| < 4$ is used, as all of the models overestimate the width of the jet fragmentation peak. Under proper normalization, the choice of long-range definition does not affect the comparison, as the correlation is independent of $\Delta\eta$ [35] in this region, and the results can be directly compared. All models are found to underestimate the data in the examined multiplicity region, although PYTHIA with shoving and EPOS LHC do exhibit collective-like signals at $N_{ch} \gtrsim 10$ and $N_{ch} \gtrsim 24$, respectively. In contrast, the Monash tune as the no-ridge reference does not reproduce the near-side at all, and the yield remains zero across the entire multiplicity range. Only EPOS LHC describes quantitatively the magnitude of the yield at $\langle N_{ch} \rangle \geq 48$. These observations suggest that none of the models can fully capture the physics underlying the emergence of the near-side associated yield in low multiplicity pp collisions.

The high precision of this measurement allows one to draw quantitative comparisons between the ridge yield of a very small hadronic collision system to the ridge yield measured in even simpler and well

understood e^+e^- annihilations. The results presented in this Letter suggest that the ridge yield measured from a hadronic system of roughly equivalent multiplicity is non-zero and substantially larger than the limit observed in e^+e^- annihilations. Based on this, one can conclude that additional processes besides those in the e^+e^- annihilations must have role for the emergence of long-range correlations in pp collisions.

At the same time, the description of the ridge yields in well-established models is investigated. Calculations from three different models show that the ridge yield in the low multiplicity region in general is not reproduced. This suggests that the mechanisms for ridge yield production in very small hadronic collisions have not been understood and more theoretical work is needed.

Acknowledgements

The ALICE Collaboration would like to thank all its engineers and technicians for their invaluable contributions to the construction of the experiment and the CERN accelerator teams for the outstanding performance of the LHC complex. The ALICE Collaboration gratefully acknowledges the resources and support provided by all Grid centres and the Worldwide LHC Computing Grid (WLCG) collaboration. The ALICE Collaboration acknowledges the following funding agencies for their support in building and running the ALICE detector: A. I. Alikhanyan National Science Laboratory (Yerevan Physics Institute) Foundation (ANSL), State Committee of Science and World Federation of Scientists (WFS), Armenia; Austrian Academy of Sciences, Austrian Science Fund (FWF): [M 2467-N36] and Nationalstiftung für Forschung, Technologie und Entwicklung, Austria; Ministry of Communications and High Technologies, National Nuclear Research Center, Azerbaijan; Conselho Nacional de Desenvolvimento Científico e Tecnológico (CNPq), Financiadora de Estudos e Projetos (Finep), Fundação de Amparo à Pesquisa do Estado de São Paulo (FAPESP) and Universidade Federal do Rio Grande do Sul (UFRGS), Brazil; Bulgarian Ministry of Education and Science, within the National Roadmap for Research Infrastructures 2020-2027 (object CERN), Bulgaria; Ministry of Education of China (MOEC) , Ministry of Science & Technology of China (MSTC) and National Natural Science Foundation of China (NSFC), China; Ministry of Science and Education and Croatian Science Foundation, Croatia; Centro de Aplicaciones Tecnológicas y Desarrollo Nuclear (CEADEN), Cubaenergía, Cuba; Ministry of Education, Youth and Sports of the Czech Republic, Czech Republic; The Danish Council for Independent Research | Natural Sciences, the VILLUM FONDEN and Danish National Research Foundation (DNRF), Denmark; Helsinki Institute of Physics (HIP), Finland; Commissariat à l’Energie Atomique (CEA) and Institut National de Physique Nucléaire et de Physique des Particules (IN2P3) and Centre National de la Recherche Scientifique (CNRS), France; Bundesministerium für Bildung und Forschung (BMBF) and GSI Helmholtzzentrum für Schwerionenforschung GmbH, Germany; General Secretariat for Research and Technology, Ministry of Education, Research and Religions, Greece; National Research, Development and Innovation Office, Hungary; Department of Atomic Energy Government of India (DAE), Department of Science and Technology, Government of India (DST), University Grants Commission, Government of India (UGC) and Council of Scientific and Industrial Research (CSIR), India; National Research and Innovation Agency - BRIN, Indonesia; Istituto Nazionale di Fisica Nucleare (INFN), Italy; Japanese Ministry of Education, Culture, Sports, Science and Technology (MEXT) and Japan Society for the Promotion of Science (JSPS) KAKENHI, Japan; Consejo Nacional de Ciencia (CONACYT) y Tecnología, through Fondo de Cooperación Internacional en Ciencia y Tecnología (FONCICYT) and Dirección General de Asuntos del Personal Académico (DGAPA), Mexico; Nederlandse Organisatie voor Wetenschappelijk Onderzoek (NWO), Netherlands; The Research Council of Norway, Norway; Commission on Science and Technology for Sustainable Development in the South (COMSATS), Pakistan; Pontificia Universidad Católica del Perú, Peru; Ministry of Education and Science, National Science Centre and WUT ID-UB, Poland; Korea Institute of Science and Technology Information and National Research Foundation of Korea (NRF), Republic of Korea; Ministry of Education and Scientific Research,

Institute of Atomic Physics, Ministry of Research and Innovation and Institute of Atomic Physics and Universitatea Nationala de Stiinta si Tehnologie Politehnica Bucuresti, Romania; Ministry of Education, Science, Research and Sport of the Slovak Republic, Slovakia; National Research Foundation of South Africa, South Africa; Swedish Research Council (VR) and Knut & Alice Wallenberg Foundation (KAW), Sweden; European Organization for Nuclear Research, Switzerland; Suranaree University of Technology (SUT), National Science and Technology Development Agency (NSTDA) and National Science, Research and Innovation Fund (NSRF via PMU-B B05F650021), Thailand; National Academy of Sciences of Ukraine, Ukraine; Science and Technology Facilities Council (STFC), United Kingdom; National Science Foundation of the United States of America (NSF) and United States Department of Energy, Office of Nuclear Physics (DOE NP), United States of America. In addition, individual groups or members have received support from: European Research Council, Strong 2020 - Horizon 2020 (grant nos. 950692, 824093), European Union; Academy of Finland (Center of Excellence in Quark Matter) (grant nos. 346327, 346328), Finland.

References

- [1] **STAR** Collaboration, J. Adams *et al.*, “Experimental and theoretical challenges in the search for the quark gluon plasma: The STAR Collaboration’s critical assessment of the evidence from RHIC collisions”, *Nucl. Phys.* **A757** (2005) 102–183, arXiv:nucl-ex/0501009 [nucl-ex].
- [2] **PHENIX** Collaboration, K. Adcox *et al.*, “Formation of dense partonic matter in relativistic nucleus-nucleus collisions at RHIC: Experimental evaluation by the PHENIX collaboration”, *Nucl. Phys.* **A757** (2005) 184–283, arXiv:nucl-ex/0410003 [nucl-ex].
- [3] **BRAHMS** Collaboration, I. Arsene *et al.*, “Quark gluon plasma and color glass condensate at RHIC? The Perspective from the BRAHMS experiment”, *Nucl. Phys.* **A757** (2005) 1–27, arXiv:nucl-ex/0410020 [nucl-ex].
- [4] **PHOBOS** Collaboration, B. B. Back *et al.*, “The PHOBOS perspective on discoveries at RHIC”, *Nucl. Phys.* **A757** (2005) 28–101, arXiv:nucl-ex/0410022 [nucl-ex].
- [5] **ALICE** Collaboration, B. Abelev *et al.*, “Anisotropic flow of charged hadrons, pions and (anti-)protons measured at high transverse momentum in Pb–Pb collisions at $\sqrt{s_{\text{NN}}}=2.76 \text{ TeV}$ ”, *Phys. Lett. B* **719** (2013) 18–28, arXiv:1205.5761 [nucl-ex].
- [6] **ALICE** Collaboration, B. Abelev *et al.*, “Elliptic flow of identified hadrons in Pb–Pb collisions at $\sqrt{s_{\text{NN}}} = 2.76 \text{ TeV}$ ”, *JHEP* **06** (2015) 190, arXiv:1405.4632 [nucl-ex].
- [7] **ATLAS** Collaboration, G. Aad *et al.*, “Measurement of the pseudorapidity and transverse momentum dependence of the elliptic flow of charged particles in lead-lead collisions at $\sqrt{s_{\text{NN}}} = 2.76 \text{ TeV}$ with the ATLAS detector”, *Phys. Lett. B* **707** (2012) 330–348, arXiv:1108.6018 [hep-ex].
- [8] **ATLAS** Collaboration, G. Aad *et al.*, “Observation of Long-Range Elliptic Azimuthal Anisotropies in $\sqrt{s} = 13$ and 2.76 TeV pp Collisions with the ATLAS Detector”, *Phys. Rev. Lett.* **116** (2016) 172301, arXiv:1509.04776 [hep-ex].
- [9] **CMS** Collaboration, V. Khachatryan *et al.*, “Measurement of long-range near-side two-particle angular correlations in pp collisions at $\sqrt{s} = 13 \text{ TeV}$ ”, *Phys. Rev. Lett.* **116** (2016) 172302, arXiv:1510.03068 [nucl-ex].
- [10] **CMS** Collaboration, V. Khachatryan *et al.*, “Evidence for collectivity in pp collisions at the LHC”, *Phys. Lett. B* **765** (2017) 193–220, arXiv:1606.06198 [nucl-ex].

- [11] **ALICE** Collaboration, S. Acharya *et al.*, “Investigations of Anisotropic Flow Using Multiparticle Azimuthal Correlations in pp, p–Pb, Xe–Xe, and Pb–Pb Collisions at the LHC”, *Phys. Rev. Lett.* **123** (2019) 142301, arXiv:1903.01790 [nucl-ex].
- [12] **ATLAS** Collaboration, M. Aaboud *et al.*, “Measurement of long-range multiparticle azimuthal correlations with the subevent cumulant method in pp and $p + Pb$ collisions with the ATLAS detector at the CERN Large Hadron Collider”, *Phys. Rev. C* **97** (2018) 024904, arXiv:1708.03559 [hep-ex].
- [13] **ALICE** Collaboration, B. Abelev *et al.*, “Long-range angular correlations on the near and away side in p–Pb collisions at $\sqrt{s_{NN}} = 5.02$ TeV”, *Phys. Lett. B* **719** (2013) 29–41, arXiv:1212.2001 [nucl-ex].
- [14] **ATLAS** Collaboration, G. Aad *et al.*, “Measurement of long-range pseudorapidity correlations and azimuthal harmonics in $\sqrt{s_{NN}} = 5.02$ TeV proton-lead collisions with the ATLAS detector”, *Phys. Rev. C* **90** (2014) 044906, arXiv:1409.1792 [hep-ex].
- [15] **ATLAS** Collaboration, M. Aaboud *et al.*, “Measurements of long-range azimuthal anisotropies and associated Fourier coefficients for pp collisions at $\sqrt{s} = 5.02$ and 13 TeV and $p+Pb$ collisions at $\sqrt{s_{NN}} = 5.02$ TeV with the ATLAS detector”, *Phys. Rev. C* **96** (2017) 024908, arXiv:1609.06213 [nucl-ex].
- [16] **CMS** Collaboration, V. Khachatryan *et al.*, “Pseudorapidity dependence of long-range two-particle correlations in pPb collisions at $\sqrt{s_{NN}} = 5.02$ TeV”, *Phys. Rev. C* **96** (2017) 014915, arXiv:1604.05347 [nucl-ex].
- [17] **PHENIX** Collaboration, C. Aidala *et al.*, “Creation of quark–gluon plasma droplets with three distinct geometries”, *Nature Phys.* **15** (2019) 214–220, arXiv:1805.02973 [nucl-ex].
- [18] **PHENIX** Collaboration, C. Aidala *et al.*, “Measurements of Multiparticle Correlations in $d + Au$ Collisions at 200, 62.4, 39, and 19.6 GeV and $p + Au$ Collisions at 200 GeV and Implications for Collective Behavior”, *Phys. Rev. Lett.* **120** (2018) 062302, arXiv:1707.06108 [nucl-ex].
- [19] S. A. Voloshin, A. M. Poskanzer, and R. Snellings, “Collective phenomena in non-central nuclear collisions”, *Landolt-Bornstein* **23** (2010) 293–333, arXiv:0809.2949 [nucl-ex].
- [20] M. Strickland, “Small system studies: A theory overview”, *Nucl. Phys. A* **982** (2019) 92–98, arXiv:1807.07191 [nucl-th].
- [21] C. Loizides, “Experimental overview on small collision systems at the LHC”, *Nucl. Phys. A* **956** (2016) 200–207, arXiv:1602.09138 [nucl-ex].
- [22] J. L. Nagle and W. A. Zajc, “Small System Collectivity in Relativistic Hadronic and Nuclear Collisions”, *Ann. Rev. Nucl. Part. Sci.* **68** (2018) 211–235, arXiv:1801.03477 [nucl-ex].
- [23] B. Schenke, C. Shen, and P. Tribedy, “Running the gamut of high energy nuclear collisions”, *Phys. Rev. C* **102** (2020) 044905, arXiv:2005.14682 [nucl-th].
- [24] W. Zhao, S. Ryu, C. Shen, and B. Schenke, “3D structure of anisotropic flow in small collision systems at energies available at the BNL Relativistic Heavy Ion Collider”, *Phys. Rev. C* **107** (2023) 014904, arXiv:2211.16376 [nucl-th].
- [25] **STAR** Collaboration, M. I. Abdulhamid *et al.*, “Measurements of the Elliptic and Triangular Azimuthal Anisotropies in Central He3+Au, d+Au and p+Au Collisions at $\sqrt{s_{NN}} = 200$ GeV”, *Phys. Rev. Lett.* **130** (2023) 242301, arXiv:2210.11352 [nucl-ex].

- [26] K. Dusling and R. Venugopalan, “Evidence for BFKL and saturation dynamics from dihadron spectra at the LHC”, *Phys. Rev. D* **87** (2013) 051502, arXiv:1210.3890 [hep-ph].
- [27] A. Bzdak, B. Schenke, P. Tribedy, and R. Venugopalan, “Initial state geometry and the role of hydrodynamics in proton-proton, proton-nucleus and deuteron-nucleus collisions”, *Phys. Rev. C* **87** (2013) 064906, arXiv:1304.3403 [nucl-th].
- [28] M. Greif, C. Greiner, B. Schenke, S. Schlichting, and Z. Xu, “Importance of initial and final state effects for azimuthal correlations in p+Pb collisions”, *Phys. Rev. D* **96** (2017) 091504, arXiv:1708.02076 [hep-ph].
- [29] H. Mantysaari, B. Schenke, C. Shen, and P. Tribedy, “Imprints of fluctuating proton shapes on flow in proton-lead collisions at the LHC”, *Phys. Lett. B* **772** (2017) 681–686, arXiv:1705.03177 [nucl-th].
- [30] B. Schenke, S. Schlichting, and P. Singh, “Rapidity dependence of initial state geometry and momentum correlations in p+Pb collisions”, *Phys. Rev. D* **105** (2022) 094023, arXiv:2201.08864 [nucl-th].
- [31] **ALEPH** Collaboration, D. Decamp *et al.*, “Aleph: A detector for electron-positron annihilations at lep”, *Nuclear Instruments and Methods in Physics Research Section A: Accelerators, Spectrometers, Detectors and Associated Equipment* **294** (1990) 121–178. <https://www.sciencedirect.com/science/article/pii/016890029091831U>.
- [32] A. Badea, A. Baty, P. Chang, G. M. Innocenti, M. Maggi, C. McGinn, M. Peters, T.-A. Sheng, J. Thaler, and Y.-J. Lee, “Measurements of two-particle correlations in e^+e^- collisions at 91 GeV with ALEPH archived data”, *Phys. Rev. Lett.* **123** (2019) 212002, arXiv:1906.00489 [hep-ex].
- [33] J. L. Nagle, R. Belmont, K. Hill, J. O. Koop, D. V. Perepelitsa, P. Yin, Z.-W. Lin, and D. McGlinchey, “Minimal conditions for collectivity in e^+e^- and $p + p$ collisions”, *Phys. Rev. C* **97** (Feb, 2018) 024909. <https://link.aps.org/doi/10.1103/PhysRevC.97.024909>.
- [34] P. Castorina, D. Lanteri, and H. Satz, “Strangeness enhancement and flow-like effects in e^+e^- annihilation at high parton density”, *Eur. Phys. J. A* **57** (2021) 111, arXiv:2011.06966 [hep-ph].
- [35] **CMS** Collaboration, V. Khachatryan *et al.*, “Measurement of long-range near-side two-particle angular correlations in pp collisions at $\sqrt{s} = 13$ TeV”, *Phys. Rev. Lett.* **116** (2016) 172302, arXiv:1510.03068 [nucl-ex].
- [36] **CMS** Collaboration, V. Khachatryan *et al.*, “Observation of Long-Range Near-Side Angular Correlations in Proton-Proton Collisions at the LHC”, *JHEP* **09** (2010) 091, arXiv:1009.4122 [hep-ex].
- [37] A. Ortiz Velasquez, P. Christiansen, E. Cuautle Flores, I. Maldonado Cervantes, and G. Paić, “Color Reconnection and Flowlike Patterns in pp Collisions”, *Phys. Rev. Lett.* **111** (2013) 042001, arXiv:1303.6326 [hep-ph].
- [38] C. Bierlich *et al.*, “A comprehensive guide to the physics and usage of PYTHIA 8.3”, arXiv:2203.11601 [hep-ph].
- [39] H. Song, S. A. Bass, U. Heinz, T. Hirano, and C. Shen, “200 A GeV Au+Au collisions serve a nearly perfect quark-gluon liquid”, *Phys. Rev. Lett.* **106** (2011) 192301, arXiv:1011.2783 [nucl-th]. [Erratum: Phys.Rev.Lett. 109, 139904 (2012)].

- [40] T. Pierog, I. Karpenko, J. Katzy, E. Yatsenko, and K. Werner, “EPOS LHC: Test of collective hadronization with data measured at the CERN Large Hadron Collider”, *Phys. Rev. C* **92** (2015) 034906, arXiv:1306.0121 [hep-ph].
- [41] ALICE Collaboration, “The ALICE experiment – A journey through QCD”, arXiv:2211.04384 [nucl-ex].
- [42] ALICE Collaboration, K. Aamodt *et al.*, “The ALICE experiment at the CERN LHC”, *JINST* **3** (2008) S08002.
- [43] ALICE Collaboration, B. B. Abelev *et al.*, “Performance of the ALICE Experiment at the CERN LHC”, *Int. J. Mod. Phys. A* **29** (2014) 1430044, arXiv:1402.4476 [nucl-ex].
- [44] P. Skands, S. Carrazza, and J. Rojo, “Tuning PYTHIA 8.1: the Monash 2013 Tune”, *Eur. Phys. J. C* **74** (2014) 3024, arXiv:1404.5630 [hep-ph].
- [45] R. Brun, F. Bruyant, F. Carminati, S. Giani, M. Maire, A. McPherson, G. Patrick, and L. Urban, “GEANT Detector Description and Simulation Tool”,
<https://cds.cern.ch/record/1082634>.
- [46] ALICE Collaboration, S. Acharya *et al.*, “Multiplicity and event-scale dependent flow and jet fragmentation in pp collisions at $\sqrt{s} = 13$ TeV and in p–Pb collisions at $\sqrt{s_{\text{NN}}} = 5.02$ TeV”, arXiv:2308.16591 [nucl-ex].
- [47] ALICE Collaboration, S. Acharya *et al.*, “Long- and short-range correlations and their event-scale dependence in high-multiplicity pp collisions at $\sqrt{s} = 13$ TeV”, *JHEP* **05** (2021) 290, arXiv:2101.03110 [nucl-ex].
- [48] C. Bierlich, G. Gustafson, and L. Lönnblad, “Collectivity without plasma in hadronic collisions”, *Phys. Lett. B* **779** (2018) 58–63, arXiv:1710.09725 [hep-ph].

A The ALICE Collaboration

- S. Acharya ¹²⁷, D. Adamová ⁸⁶, G. Aglieri Rinella ³³, M. Agnello ³⁰, N. Agrawal ⁵², Z. Ahammed ¹³⁵, S. Ahmad ¹⁶, S.U. Ahn ⁷², I. Ahuja ³⁸, A. Akindinov ¹⁴¹, M. Al-Turany ⁹⁷, D. Aleksandrov ¹⁴¹, B. Alessandro ⁵⁷, H.M. Alfanda ⁶, R. Alfaro Molina ⁶⁸, B. Ali ¹⁶, A. Alici ²⁶, N. Alizadehvandchali ¹¹⁶, A. Alkin ³³, J. Alme ²¹, G. Alocco ⁵³, T. Alt ⁶⁵, A.R. Altamura ⁵¹, I. Altsybeev ⁹⁵, J.R. Alvarado ⁴⁵, M.N. Anaam ⁶, C. Andrei ⁴⁶, N. Andreou ¹¹⁵, A. Andronic ¹²⁶, E. Andronov ¹⁴¹, V. Anguelov ⁹⁴, F. Antinori ⁵⁵, P. Antonioli ⁵², N. Apadula ⁷⁴, L. Aphecetche ¹⁰³, H. Appelshäuser ⁶⁵, C. Arata ⁷³, S. Arcelli ²⁶, M. Aresti ²³, R. Arnaldi ⁵⁷, J.G.M.C.A. Arneiro ¹¹⁰, I.C. Arsene ²⁰, M. Arslanok ¹³⁸, A. Augustinus ³³, R. Averbeck ⁹⁷, M.D. Azmi ¹⁶, H. Baba ¹²⁴, A. Badalà ⁵⁴, J. Bae ¹⁰⁴, Y.W. Baek ⁴¹, X. Bai ¹²⁰, R. Bailhache ⁶⁵, Y. Bailung ⁴⁹, R. Bala ⁹¹, A. Balbino ³⁰, A. Baldisseri ¹³⁰, B. Balis ², D. Banerjee ⁴, Z. Banoo ⁹¹, F. Barile ³², L. Barioglio ⁵⁷, M. Barlou ⁷⁸, B. Barman ⁴², G.G. Barnaföldi ⁴⁷, L.S. Barnby ⁸⁵, E. Barreau ¹⁰³, V. Barret ¹²⁷, L. Barreto ¹¹⁰, C. Bartels ¹¹⁹, K. Barth ³³, E. Bartsch ⁶⁵, N. Bastid ¹²⁷, S. Basu ⁷⁵, G. Batigne ¹⁰³, D. Battistini ⁹⁵, B. Batyunya ¹⁴², D. Bauri ⁴⁸, J.L. Bazo Alba ¹⁰¹, I.G. Bearden ⁸³, C. Beattie ¹³⁸, P. Becht ⁹⁷, D. Behera ⁴⁹, I. Belikov ¹²⁹, A.D.C. Bell Hechavarria ¹²⁶, F. Bellini ²⁶, R. Bellwied ¹¹⁶, S. Belokurova ¹⁴¹, L.G.E. Beltran ¹⁰⁹, Y.A.V. Beltran ⁴⁵, G. Bencedi ⁴⁷, S. Beole ²⁵, Y. Berdnikov ¹⁴¹, A. Berdnikova ⁹⁴, L. Bergmann ⁹⁴, M.G. Besoiu ⁶⁴, L. Betev ³³, P.P. Bhaduri ¹³⁵, A. Bhasin ⁹¹, M.A. Bhat ⁴, B. Bhattacharjee ⁴², L. Bianchi ²⁵, N. Bianchi ⁵⁰, J. Bielčík ³⁶, J. Bielčíková ⁸⁶, A.P. Bigot ¹²⁹, A. Bilandzic ⁹⁵, G. Biro ⁴⁷, S. Biswas ⁴, N. Bize ¹⁰³, J.T. Blair ¹⁰⁸, D. Blau ¹⁴¹, M.B. Blidaru ⁹⁷, N. Bluhme ³⁹, C. Blume ⁶⁵, G. Boca ^{22,56}, F. Bock ⁸⁷, T. Bodova ²¹, S. Boi ²³, J. Bok ¹⁷, L. Boldizsár ⁴⁷, M. Bombara ³⁸, P.M. Bond ³³, G. Bonomi ^{134,56}, H. Borel ¹³⁰, A. Borissov ¹⁴¹, A.G. Borquez Carcamo ⁹⁴, H. Bossi ¹³⁸, E. Botta ²⁵, Y.E.M. Bouziani ⁶⁵, L. Bratrud ⁶⁵, P. Braun-Munzinger ⁹⁷, M. Bregant ¹¹⁰, M. Broz ³⁶, G.E. Bruno ^{96,32}, M.D. Buckland ²⁴, D. Budnikov ¹⁴¹, H. Buesching ⁶⁵, S. Bufalino ³⁰, P. Buhler ¹⁰², N. Burmasov ¹⁴¹, Z. Buthelezi ^{69,123}, A. Bylinkin ²¹, S.A. Bysiak ¹⁰⁷, J.C. Cabanillas Noris ¹⁰⁹, M. Cai ⁶, H. Caines ¹³⁸, A. Caliva ²⁹, E. Calvo Villar ¹⁰¹, J.M.M. Camacho ¹⁰⁹, P. Camerini ²⁴, F.D.M. Canedo ¹¹⁰, S.L. Cantway ¹³⁸, M. Carabas ¹¹³, A.A. Carballo ³³, F. Carnesecchi ³³, R. Caron ¹²⁸, L.A.D. Carvalho ¹¹⁰, J. Castillo Castellanos ¹³⁰, F. Catalano ^{33,25}, S. Cattaruzzi ²⁴, C. Ceballos Sanchez ¹⁴², I. Chakaberia ⁷⁴, P. Chakraborty ⁴⁸, S. Chandra ¹³⁵, S. Chapelard ³³, M. Chartier ¹¹⁹, S. Chattopadhyay ¹³⁵, S. Chattopadhyay ⁹⁹, T. Cheng ^{97,6}, C. Cheshkov ¹²⁸, V. Chibante Barroso ³³, D.D. Chinellato ¹¹¹, E.S. Chizzali ^{II,95}, J. Cho ⁵⁹, S. Cho ⁵⁹, P. Chochula ³³, D. Choudhury ⁴², P. Christakoglou ⁸⁴, C.H. Christensen ⁸³, P. Christiansen ⁷⁵, T. Chujo ¹²⁵, M. Ciacco ³⁰, C. Cicalo ⁵³, M.R. Ciupek ⁹⁷, G. Clai^{III,52}, F. Colamaria ⁵¹, J.S. Colburn ¹⁰⁰, D. Colella ^{96,32}, M. Colocci ²⁶, M. Concas ^{IV,33}, G. Conesa Balbastre ⁷³, Z. Conesa del Valle ¹³¹, G. Contin ²⁴, J.G. Contreras ³⁶, M.L. Coquet ¹³⁰, P. Cortese ^{133,57}, M.R. Cosentino ¹¹², F. Costa ³³, S. Costanza ^{22,56}, C. Cot ¹³¹, J. Crkovská ⁹⁴, P. Crochet ¹²⁷, R. Cruz-Torres ⁷⁴, P. Cui ⁶, A. Dainese ⁵⁵, M.C. Danisch ⁹⁴, A. Danu ⁶⁴, P. Das ⁸⁰, P. Das ⁴, S. Das ⁴, A.R. Dash ¹²⁶, S. Dash ⁴⁸, A. De Caro ²⁹, G. de Cataldo ⁵¹, J. de Cuveland ³⁹, A. De Falco ²³, D. De Gruttola ²⁹, N. De Marco ⁵⁷, C. De Martin ²⁴, S. De Pasquale ²⁹, R. Deb ¹³⁴, R. Del Grande ⁹⁵, L. Dello Stritto ^{33,29}, W. Deng ⁶, P. Dhankher ¹⁹, D. Di Bari ³², A. Di Mauro ³³, B. Diab ¹³⁰, R.A. Diaz ^{142,7}, T. Dietel ¹¹⁴, Y. Ding ⁶, J. Ditzel ⁶⁵, R. Divià ³³, D.U. Dixit ¹⁹, Ø. Djuvsland ²¹, U. Dmitrieva ¹⁴¹, A. Dobrin ⁶⁴, B. Dönigus ⁶⁵, J.M. Dubinski ¹³⁶, A. Dubla ⁹⁷, S. Dudi ⁹⁰, P. Dupieux ¹²⁷, M. Durkac ¹⁰⁶, N. Dzalaiova ¹³, T.M. Eder ¹²⁶, R.J. Ehlers ⁷⁴, F. Eisenhut ⁶⁵, R. Ejima ⁹², D. Elia ⁵¹, B. Erasmus ¹⁰³, F. Ercolelli ²⁶, B. Espagnon ¹³¹, G. Eulisse ³³, D. Evans ¹⁰⁰, S. Evdokimov ¹⁴¹, L. Fabbietti ⁹⁵, M. Faggin ²⁸, J. Faivre ⁷³, F. Fan ⁶, W. Fan ⁷⁴, A. Fantoni ⁵⁰, M. Fasel ⁸⁷, A. Feliciello ⁵⁷, G. Feofilov ¹⁴¹, A. Fernández Téllez ⁴⁵, L. Ferrandi ¹¹⁰, M.B. Ferrer ³³, A. Ferrero ¹³⁰, C. Ferrero ⁵⁷, A. Ferretti ²⁵, V.J.G. Feuillard ⁹⁴, V. Filova ³⁶, D. Finogeev ¹⁴¹, F.M. Fionda ⁵³, E. Flatland ³³, F. Flor ¹¹⁶, A.N. Flores ¹⁰⁸, S. Foertsch ⁶⁹, I. Fokin ⁹⁴, S. Fokin ¹⁴¹, E. Fragiacomo ⁵⁸, E. Frajna ⁴⁷, U. Fuchs ³³, N. Funicello ²⁹, C. Furret ⁷³, A. Furs ¹⁴¹, T. Fusayasu ⁹⁸, J.J. Gaardhøje ⁸³, M. Gagliardi ²⁵, A.M. Gago ¹⁰¹, T. Gahlaud ⁴⁸, C.D. Galvan ¹⁰⁹, D.R. Gangadharan ¹¹⁶, P. Ganoti ⁷⁸, C. Garabatos ⁹⁷, T. García Chávez ⁴⁵, E. Garcia-Solis ⁹, C. Gargiulo ³³, P. Gasik ⁹⁷, A. Gautam ¹¹⁸, M.B. Gay Ducati ⁶⁷, M. Germain ¹⁰³, A. Ghimouz ¹²⁵, C. Ghosh ¹³⁵, M. Giacalone ⁵², G. Gioachin ³⁰, P. Giubellino ^{97,57}, P. Giubilato ²⁸, A.M.C. Glaenzer ¹³⁰, P. Glässel ⁹⁴, E. Glimos ¹²², D.J.Q. Goh ⁷⁶, V. Gonzalez ¹³⁷, P. Gordeev ¹⁴¹, M. Gorgon ², K. Goswami ⁴⁹, S. Gotovac ³⁴, V. Grabski ⁶⁸, L.K. Graczykowski ¹³⁶, E. Grecka ⁸⁶, A. Grelli ⁶⁰, C. Grigoras ³³, V. Grigoriev ¹⁴¹, S. Grigoryan ^{142,1}, F. Grossa ³³, J.F. Grosse-Oetringhaus ³³, R. Grossi ⁹⁷, D. Grund ³⁶, N.A. Grunwald ⁹⁴, G.G. Guardiano ¹¹¹, R. Guernane ⁷³, M. Guilbaud ¹⁰³, K. Gulbrandsen ⁸³, T. Gündem ⁶⁵, T. Gunji ¹²⁴,

- W. Guo ⁶, A. Gupta ⁹¹, R. Gupta ⁴⁹, R. Gupta ⁴⁹, K. Gwizdziel ¹³⁶, L. Gyulai ⁴⁷, C. Hadjidakis ¹³¹, F.U. Haider ⁹¹, S. Haidlova ³⁶, M. Haldar⁴, H. Hamagaki ⁷⁶, A. Hamdi ⁷⁴, Y. Han ¹³⁹, B.G. Hanley ¹³⁷, R. Hannigan ¹⁰⁸, J. Hansen ⁷⁵, J.W. Harris ¹³⁸, A. Harton ⁹, M.V. Hartung ⁶⁵, H. Hassan ¹¹⁷, D. Hatzifotiadou ⁵², P. Hauer ⁴³, L.B. Havener ¹³⁸, E. Hellbär ⁹⁷, H. Helstrup ³⁵, M. Hemmer ⁶⁵, T. Herman ³⁶, G. Herrera Corral ⁸, F. Herrmann ¹²⁶, S. Herrmann ¹²⁸, K.F. Hetland ³⁵, B. Heybeck ⁶⁵, H. Hillemanns ³³, B. Hippolyte ¹²⁹, F.W. Hoffmann ⁷¹, B. Hofman ⁶⁰, G.H. Hong ¹³⁹, M. Horst ⁹⁵, A. Horzyk ², Y. Hou ⁶, P. Hristov ³³, P. Huhn ⁶⁵, L.M. Huhta ¹¹⁷, T.J. Humanic ⁸⁸, A. Hutson ¹¹⁶, D. Hutter ³⁹, M.C. Hwang ¹⁹, R. Ilkaev ¹⁴¹, H. Ilyas ¹⁴, M. Inaba ¹²⁵, G.M. Innocenti ³³, M. Ippolitov ¹⁴¹, A. Isakov ⁸⁴, T. Isidori ¹¹⁸, M.S. Islam ⁹⁹, M. Ivanov ⁹⁷, M. Ivanov ¹³, V. Ivanov ¹⁴¹, K.E. Iversen ⁷⁵, M. Jablonski ², B. Jacak ^{19,74}, N. Jacazio ²⁶, P.M. Jacobs ⁷⁴, S. Jadlovska ¹⁰⁶, J. Jadlovsky ¹⁰⁶, S. Jaelani ⁸², C. Jahnke ¹¹⁰, M.J. Jakubowska ¹³⁶, M.A. Janik ¹³⁶, T. Janson ⁷¹, S. Ji ¹⁷, S. Jia ¹⁰, A.A.P. Jimenez ⁶⁶, F. Jonas ^{74,87,126}, D.M. Jones ¹¹⁹, J.M. Jowett ^{33,97}, J. Jung ⁶⁵, M. Jung ⁶⁵, A. Junique ³³, A. Jusko ¹⁰⁰, M.J. Kabus ^{33,136}, J. Kaewjai ¹⁰⁵, P. Kalinak ⁶¹, A.S. Kalteyer ⁹⁷, A. Kalweit ³³, D. Karatovic ⁸⁹, O. Karavichev ¹⁴¹, T. Karavicheva ¹⁴¹, P. Karczmarczyk ¹³⁶, E. Karpechev ¹⁴¹, U. Kebschull ⁷¹, R. Keidel ¹⁴⁰, D.L.D. Keijdener ⁶⁰, M. Keil ³³, B. Ketzer ⁴³, S.S. Khade ⁴⁹, A.M. Khan ¹²⁰, S. Khan ¹⁶, A. Khanzadeev ¹⁴¹, Y. Kharlov ¹⁴¹, A. Khatun ¹¹⁸, A. Khuntia ³⁶, Z. Khuranova ⁶⁵, B. Kileng ³⁵, B. Kim ¹⁰⁴, C. Kim ¹⁷, D.J. Kim ¹¹⁷, E.J. Kim ⁷⁰, J. Kim ¹³⁹, J. Kim ⁵⁹, J. Kim ⁷⁰, M. Kim ¹⁹, S. Kim ¹⁸, T. Kim ¹³⁹, K. Kimura ⁹², S. Kirsch ⁶⁵, I. Kisiel ³⁹, S. Kiselev ¹⁴¹, A. Kisiel ¹³⁶, J.P. Kitowski ², J.L. Klay ⁵, J. Klein ³³, S. Klein ⁷⁴, C. Klein-Bösing ¹²⁶, M. Kleiner ⁶⁵, T. Klemenz ⁹⁵, A. Kluge ³³, C. Kobdaj ¹⁰⁵, T. Kollegger ⁹⁷, A. Kondratyev ¹⁴², N. Kondratyeva ¹⁴¹, J. Konig ⁶⁵, S.A. Konigstorfer ⁹⁵, P.J. Konopka ³³, G. Kornakov ¹³⁶, M. Korwieser ⁹⁵, S.D. Koryciak ², A. Kotliarov ⁸⁶, N. Kovacic ⁸⁹, V. Kovalenko ¹⁴¹, M. Kowalski ¹⁰⁷, V. Kozhuharov ³⁷, I. Králik ⁶¹, A. Kravčáková ³⁸, L. Krcal ^{33,39}, M. Krivda ^{100,61}, F. Krizek ⁸⁶, K. Krizkova Gajdosova ³³, M. Kroesen ⁹⁴, M. Krüger ⁶⁵, D.M. Krupova ³⁶, E. Kryshen ¹⁴¹, V. Kučera ⁵⁹, C. Kuhn ¹²⁹, P.G. Kuijer ⁸⁴, T. Kumaoka ¹²⁵, D. Kumar ¹³⁵, L. Kumar ⁹⁰, N. Kumar ⁹⁰, S. Kumar ³², S. Kundu ³³, P. Kurashvili ⁷⁹, A. Kurepin ¹⁴¹, A.B. Kurepin ¹⁴¹, A. Kuryakin ¹⁴¹, S. Kushpil ⁸⁶, V. Kuskov ¹⁴¹, M. Kutyla ¹³⁶, M.J. Kweon ⁵⁹, Y. Kwon ¹³⁹, S.L. La Pointe ³⁹, P. La Rocca ²⁷, A. Lakrathok ¹⁰⁵, M. Lamanna ³³, A.R. Landou ⁷³, R. Langoy ¹²¹, P. Larionov ³³, E. Laudi ³³, L. Lautner ^{33,95}, R. Lavicka ¹⁰², R. Lea ^{134,56}, H. Lee ¹⁰⁴, I. Legrand ⁴⁶, G. Legras ¹²⁶, J. Lehrbach ³⁹, T.M. Lelek ², R.C. Lemmon ⁸⁵, I. León Monzón ¹⁰⁹, M.M. Lesch ⁹⁵, E.D. Lesser ¹⁹, P. Lévai ⁴⁷, X. Li ¹⁰, B.E. Liang-gilman ¹⁹, J. Lien ¹²¹, R. Lietava ¹⁰⁰, I. Likmeta ¹¹⁶, B. Lim ²⁵, S.H. Lim ¹⁷, V. Lindenstruth ³⁹, A. Lindner ⁴⁶, C. Lippmann ⁹⁷, D.H. Liu ⁶, J. Liu ¹¹⁹, G.S.S. Liveraro ¹¹¹, I.M. Lofnes ²¹, C. Loizides ⁸⁷, S. Lokos ¹⁰⁷, J. Lomker ⁶⁰, P. Loncar ³⁴, X. Lopez ¹²⁷, E. López Torres ⁷, P. Lu ^{97,120}, F.V. Lugo ⁶⁸, J.R. Luhder ¹²⁶, M. Lunardon ²⁸, G. Luparello ⁵⁸, Y.G. Ma ⁴⁰, M. Mager ³³, A. Maire ¹²⁹, E.M. Majerz ², M.V. Makariev ³⁷, M. Malaev ¹⁴¹, G. Malfattore ²⁶, N.M. Malik ⁹¹, Q.W. Malik ²⁰, S.K. Malik ⁹¹, L. Malinina ^{I,VII,142}, D. Mallick ¹³¹, N. Mallick ⁴⁹, G. Mandaglio ^{31,54}, S.K. Mandal ⁷⁹, V. Manko ¹⁴¹, F. Manso ¹²⁷, V. Manzari ⁵¹, Y. Mao ⁶, R.W. Marcjan ², G.V. Margagliotti ²⁴, A. Margotti ⁵², A. Marín ⁹⁷, C. Markert ¹⁰⁸, P. Martinengo ³³, M.I. Martínez ⁴⁵, G. Martínez García ¹⁰³, M.P.P. Martins ¹¹⁰, S. Masciocchi ⁹⁷, M. Masera ²⁵, A. Masoni ⁵³, L. Massacrier ¹³¹, O. Massen ⁶⁰, A. Mastroserio ^{132,51}, O. Matonoha ⁷⁵, S. Mattiazzo ²⁸, A. Matyja ¹⁰⁷, C. Mayer ¹⁰⁷, A.L. Mazuecos ³³, F. Mazzaschi ²⁵, M. Mazzilli ³³, J.E. Mdhului ¹²³, Y. Melikyan ⁴⁴, A. Menchaca-Rocha ⁶⁸, J.E.M. Mendez ⁶⁶, E. Meninno ¹⁰², A.S. Menon ¹¹⁶, M. Meres ¹³, Y. Miake ¹²⁵, L. Micheletti ³³, D.L. Mihaylov ⁹⁵, K. Mikhaylov ^{142,141}, D. Miśkowiec ⁹⁷, A. Modak ⁴, B. Mohanty ⁸⁰, M. Mohisin Khan ^{V,16}, M.A. Molander ⁴⁴, S. Monira ¹³⁶, C. Mordasini ¹¹⁷, D.A. Moreira De Godoy ¹²⁶, I. Morozov ¹⁴¹, A. Morsch ³³, T. Mrnjavac ³³, V. Muccifora ⁵⁰, S. Muhuri ¹³⁵, J.D. Mulligan ⁷⁴, A. Mulliri ²³, M.G. Munhoz ¹¹⁰, R.H. Munzer ⁶⁵, H. Murakami ¹²⁴, S. Murray ¹¹⁴, L. Musa ³³, J. Musinsky ⁶¹, J.W. Myrcha ¹³⁶, B. Naik ¹²³, A.I. Nambrath ¹⁹, B.K. Nandi ⁴⁸, R. Nania ⁵², E. Nappi ⁵¹, A.F. Nassirpour ¹⁸, A. Nath ⁹⁴, C. Natrass ¹²², M.N. Naydenov ³⁷, A. Neagu ²⁰, A. Negru ¹¹³, E. Nekrasova ¹⁴¹, L. Nellen ⁶⁶, R. Nepeivoda ⁷⁵, S. Nese ²⁰, G. Neskovic ³⁹, N. Nicassio ⁵¹, B.S. Nielsen ⁸³, E.G. Nielsen ⁸³, S. Nikolaev ¹⁴¹, S. Nikulin ¹⁴¹, V. Nikulin ¹⁴¹, F. Noferini ⁵², S. Noh ¹², P. Nomokonov ¹⁴², J. Norman ¹¹⁹, N. Novitzky ⁸⁷, P. Nowakowski ¹³⁶, A. Nyanin ¹⁴¹, J. Nystrand ²¹, S. Oh ¹⁸, A. Ohlson ⁷⁵, V.A. Okorokov ¹⁴¹, J. Oleniacz ¹³⁶, A. Onnerstad ¹¹⁷, C. Oppedisano ⁵⁷, A. Ortiz Velasquez ⁶⁶, J. Otwinowski ¹⁰⁷, M. Oya ⁹², K. Oyama ⁷⁶, Y. Pachmayer ⁹⁴, S. Padhan ⁴⁸, D. Pagano ^{134,56}, G. Paić ⁶⁶, S. Paisano-Guzmán ⁴⁵, A. Palasciano ⁵¹, S. Panebianco ¹³⁰, H. Park ¹²⁵, H. Park ¹⁰⁴, J. Park ⁵⁹, J.E. Parkkila ³³, Y. Patley ⁴⁸, B. Paul ²³, M.M.D.M. Paulino ¹¹⁰,

- H. Pei ⁶, T. Peitzmann ⁶⁰, X. Peng ¹¹, M. Pennisi ²⁵, S. Perciballi ²⁵, D. Peresunko ¹⁴¹, G.M. Perez ⁷, Y. Pestov¹⁴¹, V. Petrov ¹⁴¹, M. Petrovici ⁴⁶, R.P. Pezzi ^{103,67}, S. Piano ⁵⁸, M. Pikna ¹³, P. Pillot ¹⁰³, O. Pinazza ^{52,33}, L. Pinsky ¹¹⁶, C. Pinto ⁹⁵, S. Pisano ⁵⁰, M. Płoskoń ⁷⁴, M. Planinic ⁸⁹, F. Pliquet ⁶⁵, M.G. Poghosyan ⁸⁷, B. Polichtchouk ¹⁴¹, S. Politano ³⁰, N. Poljak ⁸⁹, A. Pop ⁴⁶, S. Porteboeuf-Houssais ¹²⁷, V. Pozdniakov ¹⁴², I.Y. Pozos ⁴⁵, K.K. Pradhan ⁴⁹, S.K. Prasad ⁴, S. Prasad ⁴⁹, R. Preghenella ⁵², F. Prino ⁵⁷, C.A. Pruneau ¹³⁷, I. Pshenichnov ¹⁴¹, M. Puccio ³³, S. Pucillo ²⁵, Z. Pugelova ¹⁰⁶, S. Qiu ⁸⁴, L. Quaglia ²⁵, S. Ragoni ¹⁵, A. Rai ¹³⁸, A. Rakotozafindrabe ¹³⁰, L. Ramello ^{133,57}, F. Rami ¹²⁹, T.A. Rancien ⁷³, M. Rasa ²⁷, S.S. Räsänen ⁴⁴, R. Rath ⁵², M.P. Rauch ²¹, I. Ravasenga ³³, K.F. Read ^{87,122}, C. Reckziegel ¹¹², A.R. Redelbach ³⁹, K. Redlich ^{VI,79}, C.A. Reetz ⁹⁷, H.D. Regules-Medel ⁴⁵, A. Rehman ²¹, F. Reidt ³³, H.A. Reme-Ness ³⁵, Z. Rescakova ³⁸, K. Reygers ⁹⁴, A. Riabov ¹⁴¹, V. Riabov ¹⁴¹, R. Ricci ²⁹, M. Richter ²⁰, A.A. Riedel ⁹⁵, W. Riegler ³³, A.G. Riffero ²⁵, C. Ristea ⁶⁴, M.V. Rodriguez ³³, M. Rodríguez Cahuantzi ⁴⁵, S.A. Rodríguez Ramírez ⁴⁵, K. Røed ²⁰, R. Rogalev ¹⁴¹, E. Rogochaya ¹⁴², T.S. Rogoschinski ⁶⁵, D. Rohr ³³, D. Röhrich ²¹, P.F. Rojas ⁴⁵, S. Rojas Torres ³⁶, P.S. Rokita ¹³⁶, G. Romanenko ²⁶, F. Ronchetti ⁵⁰, A. Rosano ^{31,54}, E.D. Rosas ⁶⁶, K. Roslon ¹³⁶, A. Rossi ⁵⁵, A. Roy ⁴⁹, S. Roy ⁴⁸, N. Rubini ²⁶, D. Ruggiano ¹³⁶, R. Rui ²⁴, P.G. Russek ², R. Russo ⁸⁴, A. Rustamov ⁸¹, E. Ryabinkin ¹⁴¹, Y. Ryabov ¹⁴¹, A. Rybicki ¹⁰⁷, H. Rytkonen ¹¹⁷, J. Ryu ¹⁷, W. Rzesz ¹³⁶, O.A.M. Saarimaki ⁴⁴, S. Sadhu ³², S. Sadovsky ¹⁴¹, J. Saetre ²¹, K. Šafařík ³⁶, P. Saha ⁴², S.K. Saha ⁴, S. Saha ⁸⁰, B. Sahoo ⁴⁹, R. Sahoo ⁴⁹, S. Sahoo ⁶², D. Sahu ⁴⁹, P.K. Sahu ⁶², J. Saini ¹³⁵, K. Sajdakova ³⁸, S. Sakai ¹²⁵, M.P. Salvan ⁹⁷, S. Sambyal ⁹¹, D. Samitz ¹⁰², I. Sanna ^{33,95}, T.B. Saramela ¹¹⁰, D. Sarkar ⁸³, P. Sarma ⁴², V. Sarritzu ²³, V.M. Sarti ⁹⁵, M.H.P. Sas ³³, S. Sawan ⁸⁰, E. Scapparone ⁵², J. Schambach ⁸⁷, H.S. Scheid ⁶⁵, C. Schiaua ⁴⁶, R. Schicker ⁹⁴, F. Schlepper ⁹⁴, A. Schmah ⁹⁷, C. Schmidt ⁹⁷, H.R. Schmidt ⁹³, M.O. Schmidt ³³, M. Schmidt ⁹³, N.V. Schmidt ⁸⁷, A.R. Schmier ¹²², R. Schotter ¹²⁹, A. Schröter ³⁹, J. Schukraft ³³, K. Schweda ⁹⁷, G. Scioli ²⁶, E. Scomparin ⁵⁷, J.E. Seger ¹⁵, Y. Sekiguchi ¹²⁴, D. Sekihata ¹²⁴, M. Selina ⁸⁴, I. Selyuzhenkov ⁹⁷, S. Senyukov ¹²⁹, J.J. Seo ⁹⁴, D. Serebryakov ¹⁴¹, L. Serkin ⁶⁶, L. Šerkšnytė ⁹⁵, A. Sevcenco ⁶⁴, T.J. Shaba ⁶⁹, A. Shabetai ¹⁰³, R. Shahoyan ³³, A. Shangaraev ¹⁴¹, B. Sharma ⁹¹, D. Sharma ⁴⁸, H. Sharma ⁵⁵, M. Sharma ⁹¹, S. Sharma ⁷⁶, S. Sharma ⁹¹, U. Sharma ⁹¹, A. Shatat ¹³¹, O. Sheibani ¹¹⁶, K. Shigaki ⁹², M. Shimomura ⁷⁷, J. Shin ¹², S. Shirinkin ¹⁴¹, Q. Shou ⁴⁰, Y. Sibirski ¹⁴¹, S. Siddhanta ⁵³, T. Siemiaczuk ⁷⁹, T.F. Silva ¹¹⁰, D. Silvermyr ⁷⁵, T. Simantathammakul ¹⁰⁵, R. Simeonov ³⁷, B. Singh ⁹¹, B. Singh ⁹⁵, K. Singh ⁴⁹, R. Singh ⁸⁰, R. Singh ⁹¹, R. Singh ⁴⁹, S. Singh ¹⁶, V.K. Singh ¹³⁵, V. Singhal ¹³⁵, T. Sinha ⁹⁹, B. Sitar ¹³, M. Sitta ^{133,57}, T.B. Skaali ²⁰, G. Skorodumovs ⁹⁴, M. Slupecki ⁴⁴, N. Smirnov ¹³⁸, R.J.M. Snellings ⁶⁰, E.H. Solheim ²⁰, J. Song ¹⁷, C. Sonnabend ^{33,97}, J.M. Sonneveld ⁸⁴, F. Soramel ²⁸, A.B. Soto-hernandez ⁸⁸, R. Spijkers ⁸⁴, I. Sputowska ¹⁰⁷, J. Staa ⁷⁵, J. Stachel ⁹⁴, I. Stan ⁶⁴, P.J. Steffanic ¹²², S.F. Stiefelmaier ⁹⁴, D. Stocco ¹⁰³, I. Storehaug ²⁰, P. Stratmann ¹²⁶, S. Strazzi ²⁶, A. Sturniolo ^{31,54}, C.P. Stylianidis ⁸⁴, A.A.P. Suaide ¹¹⁰, C. Suire ¹³¹, M. Sukhanov ¹⁴¹, M. Suljic ³³, R. Sultanov ¹⁴¹, V. Sumberia ⁹¹, S. Sumowidagdo ⁸², I. Szarka ¹³, M. Szymkowski ¹³⁶, S.F. Taghavi ⁹⁵, G. Taillepied ⁹⁷, J. Takahashi ¹¹¹, G.J. Tambave ⁸⁰, S. Tang ⁶, Z. Tang ¹²⁰, J.D. Tapia Takaki ¹¹⁸, N. Tapus ¹¹³, L.A. Tarasovicova ¹²⁶, M.G. Tarzila ⁴⁶, G.F. Tassielli ³², A. Tauro ³³, A. Tavira García ¹³¹, G. Tejeda Muñoz ⁴⁵, A. Telesca ³³, L. Terlizzi ²⁵, C. Terrevoli ¹¹⁶, S. Thakur ⁴, D. Thomas ¹⁰⁸, A. Tikhonov ¹⁴¹, N. Tiltmann ^{33,126}, A.R. Timmins ¹¹⁶, M. Tkacik ¹⁰⁶, T. Tkacik ¹⁰⁶, A. Toia ⁶⁵, R. Tokumoto ⁹², K. Tomohiro ⁹², N. Topilskaya ¹⁴¹, M. Toppi ⁵⁰, T. Tork ¹³¹, P.V. Torres ⁶⁶, V.V. Torres ¹⁰³, A.G. Torres Ramos ³², A. Trifiró ^{31,54}, A.S. Triolo ^{33,31,54}, S. Tripathy ⁵², T. Tripathy ⁴⁸, S. Trogolo ³³, V. Trubnikov ³, W.H. Trzaska ¹¹⁷, T.P. Trzcinski ¹³⁶, A. Tumkin ¹⁴¹, R. Turrisi ⁵⁵, T.S. Tveter ²⁰, K. Ullaland ²¹, B. Ulukutlu ⁹⁵, A. Uras ¹²⁸, M. Urioni ¹³⁴, G.L. Usai ²³, M. Vala ³⁸, N. Valle ²², L.V.R. van Doremalen ⁶⁰, M. van Leeuwen ⁸⁴, C.A. van Veen ⁹⁴, R.J.G. van Weelden ⁸⁴, P. Vande Vyvre ³³, D. Varga ⁴⁷, Z. Varga ⁴⁷, M. Vasileiou ⁷⁸, A. Vasiliev ¹⁴¹, O. Vázquez Doce ⁵⁰, O. Vazquez Rueda ¹¹⁶, V. Vechernin ¹⁴¹, E. Vercellin ²⁵, S. Vergara Limón ⁴⁵, R. Verma ⁴⁸, L. Vermunt ⁹⁷, R. Vértesi ⁴⁷, M. Verweij ⁶⁰, L. Vickovic ³⁴, Z. Vilakazi ¹²³, O. Villalobos Baillie ¹⁰⁰, A. Villani ²⁴, A. Vinogradov ¹⁴¹, T. Virgili ²⁹, M.M.O. Virta ¹¹⁷, V. Vislavicius ⁷⁵, A. Vodopyanov ¹⁴², B. Volkel ³³, M.A. Völk ⁹⁴, S.A. Voloshin ¹³⁷, G. Volpe ³², B. von Haller ³³, I. Vorobyev ³³, N. Vozniuk ¹⁴¹, J. Vrláková ³⁸, J. Wan ⁴⁰, C. Wang ⁴⁰, D. Wang ⁴⁰, Y. Wang ⁴⁰, Y. Wang ⁶, A. Wegrzynek ³³, F.T. Weiglhofer ³⁹, S.C. Wenzel ³³, J.P. Wessels ¹²⁶, J. Wiechula ⁶⁵, J. Wikne ²⁰, G. Wilk ⁷⁹, J. Wilkinson ⁹⁷, G.A. Willems ¹²⁶, B. Windelband ⁹⁴, M. Winn ¹³⁰, J.R. Wright ¹⁰⁸, W. Wu ⁴⁰, Y. Wu ¹²⁰, R. Xu ⁶, A. Yadav ⁴³, A.K. Yadav ¹³⁵, Y. Yamaguchi ⁹², S. Yang ²¹, S. Yano ⁹², E.R. Yeats ¹⁹, Z. Yin ⁶, I.-K. Yoo ¹⁷, J.H. Yoon ⁵⁹, H. Yu ¹², S. Yuan ²¹, A. Yuncu ⁹⁴, V. Zaccolo ²⁴,

C. Zampolli ³³, F. Zanone ⁹⁴, N. Zardoshti ³³, A. Zarochentsev ¹⁴¹, P. Závada ⁶³, N. Zaviyalov ¹⁴¹, M. Zhalov ¹⁴¹, B. Zhang ⁶, C. Zhang ¹³⁰, L. Zhang ⁴⁰, S. Zhang ⁴⁰, X. Zhang ⁶, Y. Zhang ¹²⁰, Z. Zhang ⁶, M. Zhao ¹⁰, V. Zhrebchevskii ¹⁴¹, Y. Zhi ¹⁰, C. Zhong ⁴⁰, D. Zhou ⁶, Y. Zhou ⁸³, J. Zhu ^{55,6}, Y. Zhu ⁶, S.C. Zugravel ⁵⁷, N. Zurlo ^{134,56}

Affiliation Notes

^I Deceased

^{II} Also at: Max-Planck-Institut für Physik, Munich, Germany

^{III} Also at: Italian National Agency for New Technologies, Energy and Sustainable Economic Development (ENEA), Bologna, Italy

^{IV} Also at: Dipartimento DET del Politecnico di Torino, Turin, Italy

^V Also at: Department of Applied Physics, Aligarh Muslim University, Aligarh, India

^{VI} Also at: Institute of Theoretical Physics, University of Wrocław, Poland

^{VII} Also at: An institution covered by a cooperation agreement with CERN

Collaboration Institutes

¹ A.I. Alikhanyan National Science Laboratory (Yerevan Physics Institute) Foundation, Yerevan, Armenia

² AGH University of Krakow, Cracow, Poland

³ Bogolyubov Institute for Theoretical Physics, National Academy of Sciences of Ukraine, Kiev, Ukraine

⁴ Bose Institute, Department of Physics and Centre for Astroparticle Physics and Space Science (CAPSS), Kolkata, India

⁵ California Polytechnic State University, San Luis Obispo, California, United States

⁶ Central China Normal University, Wuhan, China

⁷ Centro de Aplicaciones Tecnológicas y Desarrollo Nuclear (CEADEN), Havana, Cuba

⁸ Centro de Investigación y de Estudios Avanzados (CINVESTAV), Mexico City and Mérida, Mexico

⁹ Chicago State University, Chicago, Illinois, United States

¹⁰ China Institute of Atomic Energy, Beijing, China

¹¹ China University of Geosciences, Wuhan, China

¹² Chungbuk National University, Cheongju, Republic of Korea

¹³ Comenius University Bratislava, Faculty of Mathematics, Physics and Informatics, Bratislava, Slovak Republic

¹⁴ COMSATS University Islamabad, Islamabad, Pakistan

¹⁵ Creighton University, Omaha, Nebraska, United States

¹⁶ Department of Physics, Aligarh Muslim University, Aligarh, India

¹⁷ Department of Physics, Pusan National University, Pusan, Republic of Korea

¹⁸ Department of Physics, Sejong University, Seoul, Republic of Korea

¹⁹ Department of Physics, University of California, Berkeley, California, United States

²⁰ Department of Physics, University of Oslo, Oslo, Norway

²¹ Department of Physics and Technology, University of Bergen, Bergen, Norway

²² Dipartimento di Fisica, Università di Pavia, Pavia, Italy

²³ Dipartimento di Fisica dell’Università and Sezione INFN, Cagliari, Italy

²⁴ Dipartimento di Fisica dell’Università and Sezione INFN, Trieste, Italy

²⁵ Dipartimento di Fisica dell’Università and Sezione INFN, Turin, Italy

²⁶ Dipartimento di Fisica e Astronomia dell’Università and Sezione INFN, Bologna, Italy

²⁷ Dipartimento di Fisica e Astronomia dell’Università and Sezione INFN, Catania, Italy

²⁸ Dipartimento di Fisica e Astronomia dell’Università and Sezione INFN, Padova, Italy

²⁹ Dipartimento di Fisica ‘E.R. Caianiello’ dell’Università and Gruppo Collegato INFN, Salerno, Italy

³⁰ Dipartimento DISAT del Politecnico and Sezione INFN, Turin, Italy

³¹ Dipartimento di Scienze MIFT, Università di Messina, Messina, Italy

³² Dipartimento Interateneo di Fisica ‘M. Merlin’ and Sezione INFN, Bari, Italy

³³ European Organization for Nuclear Research (CERN), Geneva, Switzerland

³⁴ Faculty of Electrical Engineering, Mechanical Engineering and Naval Architecture, University of Split, Split, Croatia

³⁵ Faculty of Engineering and Science, Western Norway University of Applied Sciences, Bergen, Norway

- ³⁶ Faculty of Nuclear Sciences and Physical Engineering, Czech Technical University in Prague, Prague, Czech Republic
³⁷ Faculty of Physics, Sofia University, Sofia, Bulgaria
³⁸ Faculty of Science, P.J. Šafárik University, Košice, Slovak Republic
³⁹ Frankfurt Institute for Advanced Studies, Johann Wolfgang Goethe-Universität Frankfurt, Frankfurt, Germany
⁴⁰ Fudan University, Shanghai, China
⁴¹ Gangneung-Wonju National University, Gangneung, Republic of Korea
⁴² Gauhati University, Department of Physics, Guwahati, India
⁴³ Helmholtz-Institut für Strahlen- und Kernphysik, Rheinische Friedrich-Wilhelms-Universität Bonn, Bonn, Germany
⁴⁴ Helsinki Institute of Physics (HIP), Helsinki, Finland
⁴⁵ High Energy Physics Group, Universidad Autónoma de Puebla, Puebla, Mexico
⁴⁶ Horia Hulubei National Institute of Physics and Nuclear Engineering, Bucharest, Romania
⁴⁷ HUN-REN Wigner Research Centre for Physics, Budapest, Hungary
⁴⁸ Indian Institute of Technology Bombay (IIT), Mumbai, India
⁴⁹ Indian Institute of Technology Indore, Indore, India
⁵⁰ INFN, Laboratori Nazionali di Frascati, Frascati, Italy
⁵¹ INFN, Sezione di Bari, Bari, Italy
⁵² INFN, Sezione di Bologna, Bologna, Italy
⁵³ INFN, Sezione di Cagliari, Cagliari, Italy
⁵⁴ INFN, Sezione di Catania, Catania, Italy
⁵⁵ INFN, Sezione di Padova, Padova, Italy
⁵⁶ INFN, Sezione di Pavia, Pavia, Italy
⁵⁷ INFN, Sezione di Torino, Turin, Italy
⁵⁸ INFN, Sezione di Trieste, Trieste, Italy
⁵⁹ Inha University, Incheon, Republic of Korea
⁶⁰ Institute for Gravitational and Subatomic Physics (GRASP), Utrecht University/Nikhef, Utrecht, Netherlands
⁶¹ Institute of Experimental Physics, Slovak Academy of Sciences, Košice, Slovak Republic
⁶² Institute of Physics, Homi Bhabha National Institute, Bhubaneswar, India
⁶³ Institute of Physics of the Czech Academy of Sciences, Prague, Czech Republic
⁶⁴ Institute of Space Science (ISS), Bucharest, Romania
⁶⁵ Institut für Kernphysik, Johann Wolfgang Goethe-Universität Frankfurt, Frankfurt, Germany
⁶⁶ Instituto de Ciencias Nucleares, Universidad Nacional Autónoma de México, Mexico City, Mexico
⁶⁷ Instituto de Física, Universidade Federal do Rio Grande do Sul (UFRGS), Porto Alegre, Brazil
⁶⁸ Instituto de Física, Universidad Nacional Autónoma de México, Mexico City, Mexico
⁶⁹ iThemba LABS, National Research Foundation, Somerset West, South Africa
⁷⁰ Jeonbuk National University, Jeonju, Republic of Korea
⁷¹ Johann-Wolfgang-Goethe Universität Frankfurt Institut für Informatik, Fachbereich Informatik und Mathematik, Frankfurt, Germany
⁷² Korea Institute of Science and Technology Information, Daejeon, Republic of Korea
⁷³ Laboratoire de Physique Subatomique et de Cosmologie, Université Grenoble-Alpes, CNRS-IN2P3, Grenoble, France
⁷⁴ Lawrence Berkeley National Laboratory, Berkeley, California, United States
⁷⁵ Lund University Department of Physics, Division of Particle Physics, Lund, Sweden
⁷⁶ Nagasaki Institute of Applied Science, Nagasaki, Japan
⁷⁷ Nara Women's University (NWU), Nara, Japan
⁷⁸ National and Kapodistrian University of Athens, School of Science, Department of Physics , Athens, Greece
⁷⁹ National Centre for Nuclear Research, Warsaw, Poland
⁸⁰ National Institute of Science Education and Research, Homi Bhabha National Institute, Jatni, India
⁸¹ National Nuclear Research Center, Baku, Azerbaijan
⁸² National Research and Innovation Agency - BRIN, Jakarta, Indonesia
⁸³ Niels Bohr Institute, University of Copenhagen, Copenhagen, Denmark
⁸⁴ Nikhef, National institute for subatomic physics, Amsterdam, Netherlands
⁸⁵ Nuclear Physics Group, STFC Daresbury Laboratory, Daresbury, United Kingdom
⁸⁶ Nuclear Physics Institute of the Czech Academy of Sciences, Husinec-Řež, Czech Republic
⁸⁷ Oak Ridge National Laboratory, Oak Ridge, Tennessee, United States

- ⁸⁸ Ohio State University, Columbus, Ohio, United States
⁸⁹ Physics department, Faculty of science, University of Zagreb, Zagreb, Croatia
⁹⁰ Physics Department, Panjab University, Chandigarh, India
⁹¹ Physics Department, University of Jammu, Jammu, India
⁹² Physics Program and International Institute for Sustainability with Knotted Chiral Meta Matter (SKCM2), Hiroshima University, Hiroshima, Japan
⁹³ Physikalisches Institut, Eberhard-Karls-Universität Tübingen, Tübingen, Germany
⁹⁴ Physikalisches Institut, Ruprecht-Karls-Universität Heidelberg, Heidelberg, Germany
⁹⁵ Physik Department, Technische Universität München, Munich, Germany
⁹⁶ Politecnico di Bari and Sezione INFN, Bari, Italy
⁹⁷ Research Division and ExtreMe Matter Institute EMMI, GSI Helmholtzzentrum für Schwerionenforschung GmbH, Darmstadt, Germany
⁹⁸ Saga University, Saga, Japan
⁹⁹ Saha Institute of Nuclear Physics, Homi Bhabha National Institute, Kolkata, India
¹⁰⁰ School of Physics and Astronomy, University of Birmingham, Birmingham, United Kingdom
¹⁰¹ Sección Física, Departamento de Ciencias, Pontificia Universidad Católica del Perú, Lima, Peru
¹⁰² Stefan Meyer Institut für Subatomare Physik (SMI), Vienna, Austria
¹⁰³ SUBATECH, IMT Atlantique, Nantes Université, CNRS-IN2P3, Nantes, France
¹⁰⁴ Sungkyunkwan University, Suwon City, Republic of Korea
¹⁰⁵ Suranaree University of Technology, Nakhon Ratchasima, Thailand
¹⁰⁶ Technical University of Košice, Košice, Slovak Republic
¹⁰⁷ The Henryk Niewodniczanski Institute of Nuclear Physics, Polish Academy of Sciences, Cracow, Poland
¹⁰⁸ The University of Texas at Austin, Austin, Texas, United States
¹⁰⁹ Universidad Autónoma de Sinaloa, Culiacán, Mexico
¹¹⁰ Universidade de São Paulo (USP), São Paulo, Brazil
¹¹¹ Universidade Estadual de Campinas (UNICAMP), Campinas, Brazil
¹¹² Universidade Federal do ABC, Santo Andre, Brazil
¹¹³ Universitatea Națională de Știință și Tehnologie Politehnica Bucuresti, Bucharest, Romania
¹¹⁴ University of Cape Town, Cape Town, South Africa
¹¹⁵ University of Derby, Derby, United Kingdom
¹¹⁶ University of Houston, Houston, Texas, United States
¹¹⁷ University of Jyväskylä, Jyväskylä, Finland
¹¹⁸ University of Kansas, Lawrence, Kansas, United States
¹¹⁹ University of Liverpool, Liverpool, United Kingdom
¹²⁰ University of Science and Technology of China, Hefei, China
¹²¹ University of South-Eastern Norway, Kongsberg, Norway
¹²² University of Tennessee, Knoxville, Tennessee, United States
¹²³ University of the Witwatersrand, Johannesburg, South Africa
¹²⁴ University of Tokyo, Tokyo, Japan
¹²⁵ University of Tsukuba, Tsukuba, Japan
¹²⁶ Universität Münster, Institut für Kernphysik, Münster, Germany
¹²⁷ Université Clermont Auvergne, CNRS/IN2P3, LPC, Clermont-Ferrand, France
¹²⁸ Université de Lyon, CNRS/IN2P3, Institut de Physique des 2 Infinis de Lyon, Lyon, France
¹²⁹ Université de Strasbourg, CNRS, IPHC UMR 7178, F-67000 Strasbourg, France, Strasbourg, France
¹³⁰ Université Paris-Saclay, Centre d'Etudes de Saclay (CEA), IRFU, Département de Physique Nucléaire (DPhN), Saclay, France
¹³¹ Université Paris-Saclay, CNRS/IN2P3, IJCLab, Orsay, France
¹³² Università degli Studi di Foggia, Foggia, Italy
¹³³ Università del Piemonte Orientale, Vercelli, Italy
¹³⁴ Università di Brescia, Brescia, Italy
¹³⁵ Variable Energy Cyclotron Centre, Homi Bhabha National Institute, Kolkata, India
¹³⁶ Warsaw University of Technology, Warsaw, Poland
¹³⁷ Wayne State University, Detroit, Michigan, United States
¹³⁸ Yale University, New Haven, Connecticut, United States
¹³⁹ Yonsei University, Seoul, Republic of Korea
¹⁴⁰ Zentrum für Technologie und Transfer (ZTT), Worms, Germany

¹⁴¹ Affiliated with an institute covered by a cooperation agreement with CERN

¹⁴² Affiliated with an international laboratory covered by a cooperation agreement with CERN.